Observation of the Singly Cabibbo Suppressed Decay $D^0 \to b_1(1235)^- e^+ \nu_e$ and Evidence for $D^+ \to b_1(1235)^0 e^+ \nu_e$

M. Ablikim *et al.*[*]
(BESIII Collaboration)

(Received 30 July 2024; revised 7 October 2025; accepted 24 November 2025; published 13 January 2026)

By analyzing a data sample of e^+e^- collisions with center-of-mass energy $\sqrt{s} = 3.773$ GeV, corresponding to an integrated luminosity of 7.9 fb^{-1} collected with the BESIII detector operating at the BEPCII collider, we study semileptonic decays of the $D^{0(+)}$ mesons into the axial-vector meson $b_1(1235)$ via the decay $b_1(1235) \to \omega\pi$. The decay $D^0 \to b_1(1235)^- e^+ \nu_e$ is observed with a significance of 5.2σ after considering systematic uncertainty, while evidence for the decay $D^+ \to b_1(1235)^0 e^+ \nu_e$ is obtained with a 3.1σ significance. The product branching fractions are determined to be $\mathcal{B}[D^0 \to b_1(1235)^- e^+ \nu_e] \times \mathcal{B}[b_1(1235)^- \to \omega\pi^-] = (0.72 \pm 0.18^{+0.06}_{-0.08}) \times 10^{-4}$ and $\mathcal{B}[D^+ \to b_1(1235)^0 e^+ \nu_e] \times \mathcal{B}[b_1(1235)^0 \to \omega\pi^0] = (1.16 \pm 0.44 \pm 0.16) \times 10^{-4}$, where the first uncertainties are statistical and the second systematic. The ratio of their partial decay widths is determined to be $\{\Gamma[D^0 \to b_1(1235)^- e^+ \nu_e]/2\Gamma[D^+ \to b_1(1235)^0 e^+ \nu_e]\} = 0.78 \pm 0.19^{+0.04}_{-0.05}$, which is consistent with unity, predicted by isospin invariance, within uncertainties.

DOI: 10.1103/4c4g-31zx

Experimental investigations of light hadron spectroscopy in semileptonic decays of the D mesons (D denotes D^0 or D^+) can be used to shed light on the role of nonperturbative strong interactions in weak decays, thereby aiding in uncovering the internal structure of the hadrons involved. The first quantitative predictions for the partial widths of various semileptonic D decays into S- or P-wave light meson states came from the quark model developed by Isgur *et al.* (namely, ISGW) [1]. This model was later updated to include constraints from heavy quark symmetry, hyperfine distortions of wave functions, and form factors with more realistic behavior at high recoil masses (ISGW2) [2]. To date, studies of Cabibbo suppressed semileptonic D decays are not as advanced as their Cabibbo favored counterparts, which have been extensively studied both theoretically and experimentally [3–5]. In general, these decays, which are mediated by the quark level process $c \to d e^+ \nu_e$, are expected to be dominated by the ground-state pseudoscalar and vector mesons. Because of limited phase space, heavier mesons, such as P-wave states or the first radial excitations of the $d\bar{u}$ and $d\bar{d}$ mesons, are less likely to be produced. Among the heavier mesons, the most promising to be produced is the P-wave b_1 meson, which is accessible via $D \to b_1 e^+ \nu_e$. Throughout this Letter, b_1 denotes $b_1(1235)$. The ISGW2 model predicts the branching fractions of $D^0 \to b_1^- e^+ \nu_e$ and $D^+ \to b_1^0 e^+ \nu_e$ to be 1.08×10^{-4} and 1.32×10^{-4} [2], respectively. The covariant light-front quark model predicts the branching fraction of $D^+ \to b_1^0 e^+ \nu_e$ to be $(7.4 \pm 0.7) \times 10^{-5}$ [6]. The first measurements of the branching fractions of the $D^{0(+)} \to b_1^{-(0)} e^+ \nu_e$ decays help to validate these quark model predictions.

The axial-vector meson b_1, which is identified as a $^1P_1$ state in the quark model, was first observed by the HBC Collaboration in 1963 [7]. Before 1994, it was usually studied in $p\bar{p}$ [8,9], γp [10], and $p\pi$ [11–19] reactions, focusing on mass and width measurements. Later, it was widely observed in hadronic decays of D, B, and charmonium states [3]. In addition to the $q\bar{q}$ configuration, there are many different theoretical models for the nature of the b_1, such as a mixture of an ordinary $q\bar{q}$ meson and a hybrid $q\bar{q}g$ meson [20], a molecular state which is dynamically generated by the pseudoscalar-vector meson interaction [21–25], especially with strong couplings to the $K\bar{K}^*$ channel, etc. Historically, theorists and experimentalists usually considered the $\omega\pi$ decay mode to be dominant for the axial-vector b_1 meson. However, the next-to-leading order (NLO) chiral perturbation calculations [23] predict that the $\phi\pi$ channel becomes the dominant contribution under specific molecular-state assumptions. The b_1 mesons produced in semileptonic D decays offer an ideal opportunity to validate these predictions, thereby gaining insight into their nature [26]. Furthermore, compared to high backgrounds and complex interference patterns found in hadronic processes [3], the semileptonic D meson decays

[*]Full author list given at the end of the Letter.

are theoretically cleaner because leptons are not involved in strong interaction [27]. The verification of theoretical calculations of semileptonic D decays into the b_1 help to constrain the theoretical calculations in the decays of the τ [28,29], B [30–32], D [33,34], and charmonium states with b_1 involved in the final states [35–37].

To date, there is limited experimental information available on $D \to b_1 e^+ \nu_e$ decays. Only BESIII has previously searched for $D \to b_1 \ell^+ \nu_\ell$, using a portion of the same data used in this analysis, but no significant signal was obtained [38]. This Letter reports the first observation of $D^0 \to b_1^- e^+ \nu_e$ and the first evidence for $D^+ \to b_1^0 e^+ \nu_e$ with $b_1^{-(0)} \to \omega \pi^{-(0)}$, by analyzing 7.9 fb^{-1} of e^+e^- collision data taken at $\sqrt{s} = 3.773$ GeV [39]. Throughout this Letter, charge conjugate channels are always implied.

Details about the design and performance of the BESIII detector are given in Ref. [40]. The end-cap time-of-flight (TOF) system was upgraded in 2015 using multigap resistive plate chamber technology, providing a time resolution of 60 ps [41]. Approximately 63% of the data used here was collected after this upgrade. Simulated samples produced with the Geant4-based [42] Monte Carlo (MC) package which includes the geometric description of the BESIII detector and the detector response, are used to determine the detection efficiency and to estimate the backgrounds. The simulation includes the beam energy spread and initial state radiation (ISR) in the e^+e^- annihilations modeled with the generator KKMC [43]. The inclusive MC samples consist of the production of $D\bar{D}$ pairs with consideration of quantum coherence for all neutral D modes, the non-$D\bar{D}$ decays of the $\psi(3770)$, the ISR production of the J/ψ and $\psi(3686)$ states, and the continuum processes. The known decay modes are modeled with EvtGen [44] using branching fractions taken from the Particle Data Group [3], and the remaining unknown charmonium decays are estimated with Lundcharm [45]. Final state radiation from charged final state particles is incorporated using the Photos package [46]. The $D \to b_1 e^+ \nu_e$ signal MC events are simulated using the ISGW2 model [2], where the b_1 is parametrized by a relativistic Breit-Wigner function with mass and width fixed to the world-average values of 1229.5 ± 3.2 MeV/c^2 and 142 ± 9 MeV, respectively [3].

At $\sqrt{s} = 3.773$ GeV, the D and $\bar{D}$ mesons are produced in pairs without accompanying particles in the final state. Because of this, one can study semileptonic D decays with the double-tag (DT) method. Single-tag (ST) $\bar{D}^0$ mesons are first reconstructed using the hadronic decay modes $\bar{D}^0 \to K^+\pi^-$, $K^+\pi^-\pi^0$, $K^+\pi^-\pi^-\pi^+$, $K^0_S\pi^+\pi^-$, $K^+\pi^-\pi^0\pi^0$, and $K^+\pi^+\pi^-\pi^-\pi^0$; while ST D^- mesons are reconstructed via the decay modes $D^- \to K^+\pi^-\pi^-$, $K^0_S\pi^-$, $K^+\pi^-\pi^-\pi^0$, $K^0_S\pi^-\pi^0$, $K^0_S\pi^+\pi^-\pi^-$, and $K^+K^-\pi^-$. Semileptonic D candidates are then reconstructed from the residual tracks and showers not used in the tag selection. Candidate events in which the D decays into $b_1 e^+ \nu_e$ and the $\bar{D}$ decays into a tag mode are called DT events.

Because the branching fraction of the $b_1 \to \omega\pi$ decay is unknown, the product branching fractions of the decay $D \to b_1 e^+ \nu_e$ ($\mathcal{B}_{\rm SL}$) and its subsequent decay $b_1 \to \omega\pi$ ($\mathcal{B}_{b_1}$) are determined from

$$\mathcal{B}_{\rm SL} \cdot \mathcal{B}_{b_1} = \frac{N_{\rm DT}}{N^{\rm tot}_{\rm ST} \cdot \bar{\varepsilon}_{\rm SL} \cdot \mathcal{B}_{\rm sub}}, \quad (1)$$

where $N^{\rm tot}_{\rm ST} = \Sigma_i N^i_{\rm ST}$ and $N_{\rm DT}$ are the total ST and DT yields after summing over all tag modes i; $\mathcal{B}_{\rm sub} = \mathcal{B}_\omega \cdot \mathcal{B}_{\pi^0}$ for $D^0 \to b_1^- e^+ \nu_e$ and $\mathcal{B}_{\rm sub} = \mathcal{B}_\omega \cdot \mathcal{B}^2_{\pi^0}$ for $D^+ \to b_1^0 e^+ \nu_e$, in which $\mathcal{B}_\omega$ and $\mathcal{B}_{\pi^0}$ are the branching fractions of $\omega \to \pi^+\pi^-\pi^0$ and $\pi^0 \to \gamma\gamma$, respectively; and $\bar{\varepsilon}_{\rm SL} = \Sigma_i (N^i_{\rm ST}/N^{\rm tot}_{\rm ST})(\epsilon^i_{\rm DT}/\epsilon^i_{\rm ST})$ is the average signal efficiency of reconstructing $D \to b_1 e^+ \nu_e$ in the presence of an ST D, where $\epsilon^i_{\rm ST}$ and $\epsilon^i_{\rm DT}$ are the ST and DT efficiencies for the ith tag mode, respectively.

All charged tracks detected in the multilayer drift chamber (MDC) must be within a polar angle (θ) range of $|\cos\theta| < 0.93$, where θ is defined with respect to the z axis, which is the symmetry axis of the MDC. Except for charged tracks from K^0_S decays, they must originate from an interaction region defined by $|V_{xy}| < 1$ and $|V_z| < 10$ cm. Here, $|V_{xy}|$ and $|V_z|$ denote the distances of closest approach of the reconstructed track to the interaction point (IP) in the x-y plane and the z direction (along the beam), respectively. Particle identification (PID) for charged tracks combines measurements of the specific ionization energy loss in the MDC (dE/dx) and the flight time in the TOF to form confidence levels for pion and kaon hypotheses (CL_π and CL_K). Charged tracks with $\mathrm{CL}_K > \mathrm{CL}_\pi$ and $\mathrm{CL}_\pi > \mathrm{CL}_K$ are assigned as kaons and pions, respectively.

Each K^0_S candidate is reconstructed from two oppositely charged tracks satisfying $|V_z| < 20$ cm. The two charged tracks are assigned as $\pi^+\pi^-$ without imposing further PID criteria. They are constrained to originate from a common vertex and required to have an invariant mass within $(0.487, 0.511)$ GeV/c^2. The decay length of the K^0_S candidate is required to be greater than twice the vertex resolution away from the IP. The quality of the vertex fits (primary-vertex fit and secondary-vertex fit) is ensured by a requirement of $\chi^2 < 100$.

Photon candidates are selected using showers in the electromagnetic calorimeter (EMC). The deposited energy of each shower must be more than 25 MeV in the barrel region ($|\cos\theta| < 0.80$) and more than 50 MeV in the end-cap region ($0.86 < |\cos\theta| < 0.92$). To exclude showers associated with charged tracks, the angle subtended by the EMC shower and the position of the closest charged track at the EMC must be greater than 10° as measured from the IP. To suppress electronic noise and showers unrelated to the event, the difference between the EMC time and the event start time is required to be within [0, 700] ns. For π^0 candidates, the invariant mass of the photon pair is required to be within $(0.115, 0.150)$ GeV/c^2. To improve the

TABLE I. The ΔE requirements, the measured ST $\bar{D}$ yields, and the ST efficiencies ($\epsilon^i_{\rm ST}$) for different tag modes. The uncertainties are statistical only.

Tag mode	ΔE (GeV)	$N^i_{\rm ST}(\times 10^3)$	$\epsilon^i_{\rm ST}(\%)$
$\bar{D}^0 \to K^+\pi^-$	$(-0.027, 0.027)$	1449.3 ± 1.2	65.34 ± 0.01
$\bar{D}^0 \to K^+\pi^-\pi^0$	$(-0.062, 0.049)$	2913.1 ± 2.0	35.59 ± 0.01
$\bar{D}^0 \to K^+\pi^-\pi^-\pi^+$	$(-0.026, 0.024)$	1944.1 ± 1.5	40.83 ± 0.01
$\bar{D}^0 \to K^0_S\pi^+\pi^-$	$(-0.024, 0.024)$	447.6 ± 0.7	37.49 ± 0.01
$\bar{D}^0 \to K^+\pi^-\pi^0\pi^0$	$(-0.068, 0.053)$	690.6 ± 1.3	14.83 ± 0.01
$\bar{D}^0 \to K^+\pi^+\pi^-\pi^-\pi^0$	$(-0.057, 0.051)$	450.9 ± 1.1	16.17 ± 0.01
$D^- \to K^+\pi^-\pi^-$	$(-0.025, 0.024)$	2164.0 ± 1.5	51.17 ± 0.01
$D^- \to K^0_S\pi^-$	$(-0.025, 0.026)$	250.4 ± 0.5	50.74 ± 0.02
$D^- \to K^-\pi^-\pi^+\pi^0$	$(-0.057, 0.046)$	689.0 ± 1.1	25.50 ± 0.01
$D^- \to K^0_S\pi^-\pi^0$	$(-0.062, 0.049)$	558.4 ± 0.9	26.28 ± 0.01
$D^- \to K^0_S\pi^-\pi^-\pi^+$	$(-0.028, 0.027)$	300.5 ± 0.6	29.01 ± 0.01
$D^- \to K^+K^-\pi^-$	$(-0.024, 0.023)$	187.3 ± 0.5	41.06 ± 0.02

momentum resolution, a one-constraint (1C) kinematic fit to the known π^0 mass [3] is imposed on the photon pair. The four-momentum of the π^0 candidate updated by the 1C fit is kept for further analysis.

To separate the ST $\bar{D}$ mesons from combinatorial backgrounds, we define the energy difference $\Delta E \equiv E_{\bar{D}} - E_{\rm beam}$ and the beam-constrained mass $M_{\rm BC} \equiv \sqrt{E^2_{\rm beam}/c^4 - |\vec{p}_{\bar{D}}|^2/c^2}$, where $E_{\rm beam}$ is the beam energy, and $E_{\bar{D}}$ and $\vec{p}_{\bar{D}}$ are the total energy and momentum of the $\bar{D}$ candidate in the e^+e^- center-of-mass frame, respectively. If there is more than one $\bar{D}$ candidate in a given ST mode, the one with the minimal $|\Delta E|$ is kept for further analysis. The rates of multiple combinations for tag modes containing π^0 in the final state range between 8.7% and 29.0%, while those for other tag modes range between 0.1% and 7.3%. The ΔE requirements and ST efficiencies for the different tag modes are listed in Table I.

The ST yields are extracted by performing unbinned maximum likelihood fits to individual $M_{\rm BC}$ distributions. In the fit, the signal shape is derived from the MC-simulated signal shape convolved with a double Gaussian function to consider the resolution difference between data and MC simulation. The background shape is described by the ARGUS function [47], with the end point parameter fixed at 1.8865 GeV/c^2 corresponding to $E_{\rm beam}$. Figure 1 shows the fits to the $M_{\rm BC}$ distributions of the accepted ST candidates in data for different tag modes. The candidates with $M_{\rm BC}$ within $(1.859, 1.873)$ GeV/c^2 for $\bar{D}^0$ tags and $(1.863, 1.877)$ GeV/c^2 for D^- tags are kept for further analysis. Summing over the tag modes gives the total yields of ST $\bar{D}^0$ and D^- mesons to be $(7896.0 \pm 3.4_{\rm stat}) \times 10^3$ and $(4149.9 \pm 2.3_{\rm stat}) \times 10^3$, respectively.

In the presence of the tagged $\bar{D}$ candidates, $D^0 \to b_1^- e^+\nu_e$ and $D^+ \to b_1^0 e^+\nu_e$ candidates are selected from the residual tracks and photons not used in the tag reconstruction. The selection criteria of charged and neutral pions are the same as those used in the tag selection. For the

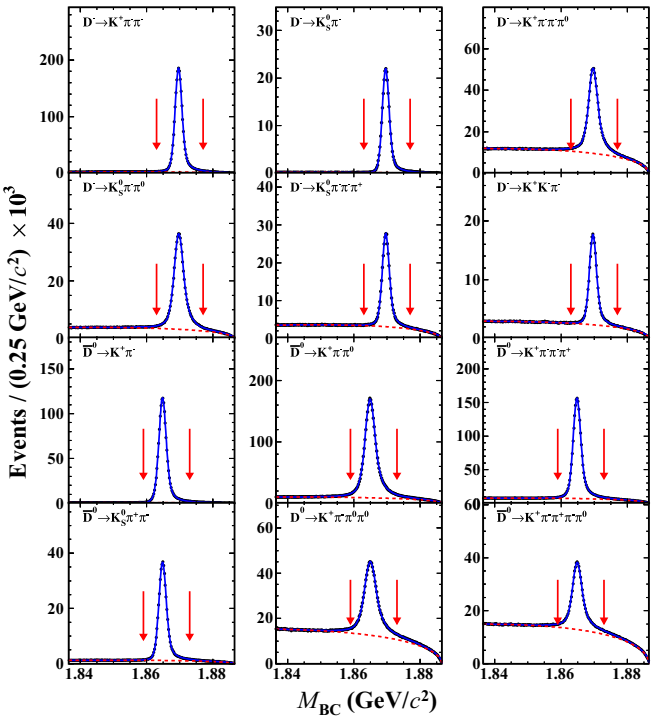

FIG. 1. Fits to the $M_{\rm BC}$ distributions of the ST $\bar{D}$ candidates for different tag modes. The dots with error bars are data, the blue curves are the best fits, and the red dashed curves are the fitted combinatorial background shapes. The pair of red arrows are the $M_{\rm BC}$ signal windows.

selected candidates $D^0 \to \pi^+\pi^-\pi^-\pi^0 e^+\nu_e$ and $D^+ \to \pi^+\pi^-\pi^0\pi^0 e^+\nu_e$, two possible $\pi^+\pi^-\pi^0$ combinations can form the ω candidate. In order to veto backgrounds from $D \to a_0(980)e^+\nu_e$, the invariant masses of both $\pi^+\pi^-\pi^0$ combinations ($M_{\pi^+\pi^-\pi^0}$) are required to be greater than 0.6 GeV/c^2. This rejects almost all of the $D \to a_0(980)e^+\nu_e$ background events. One candidate is kept for further analysis if either of the $\pi^+\pi^-\pi^0$ combinations falls in the ω mass signal region $M_{\pi^+\pi^-\pi^0} \in (0.757, 0.807)$ GeV/c^2. Events in the ω sideband region, defined as $M_{\pi^+\pi^-\pi^0} \in$ (0.697,0.742) and $(0.822, 0.867)$ GeV/c^2, are used to study potential combinatorial background in the ω signal region. To reject background events from $D^{0(+)} \to \bar{K}_1(1270)[\to K^0_S\pi^{+(0)}\pi^{-(0)}]e^+\nu_e$, we require the invariant masses of all $\pi^+\pi^-$ ($\pi^0\pi^0$) combinations satisfy $|M_{\pi^+\pi^-(\pi^0\pi^0)} - M_{K^0_S}| > 0.008$ GeV/c^2.

Identification of e^+ candidates is performed with combined dE/dx, TOF, and EMC information. Based on these, we calculate confidence levels for the positron, pion, and kaon hypotheses (CL$_e$, CL$_\pi$, and CL$_K$). Charged tracks satisfying CL$_e > 0.001$ and CL$_e$/(CL$_e$ + CL$_\pi$ + CL$_K$) > 0.8 are assigned as e^+ candidates. To further reject background events from misidentified hadrons and muons, the deposited energy of any e^+ candidate in the EMC must be

greater than 0.8 times its momentum reconstructed in the MDC.

The invariant mass of the $b_1 e^+$ system ($M_{b_1 e^+}$) is required to be less than 1.82 GeV/c^2 to suppress peaking background contributions from the decay $D \to b_1^{-(0)} \pi^+$. To suppress backgrounds with extra photons or π^0's, the maximum energy of any extra photon that has not been used in the event selection ($E^{\rm max}_{{\rm extra}\,\gamma}$) must be less than 0.30 GeV, and there must be no additional π^0 candidates ($N^{\pi^0}_{\rm extra}$) in the candidate event. In addition, the opening angle between the missing momentum and the most energetic unused shower when found, $\theta_{\gamma,{\rm miss}}$, is required to satisfy $\cos\theta_{\gamma,{\rm miss}} < 0.3$ and $\cos\theta_{\gamma,{\rm miss}} < 0.4$ for $D^0 \to b_1^- e^+ \nu_e$ and $D^+ \to b_1^0 e^+ \nu_e$, respectively. To suppress backgrounds due to final state radiation, the angle between the direction of the radiative photon and the e^+ momentum is required to be greater than 0.20 rad.

The presence of the missing neutrino is inferred using a kinematic variable defined as

$$U_{\rm miss} \equiv E_{\rm miss} - |\vec{p}_{\rm miss}| \cdot c, \tag{2}$$

with

$$E_{\rm miss} \equiv E_{\rm beam} - E_{b_1} - E_{e^+}, \tag{3}$$

and

$$\vec{p}_{\rm miss} \equiv \vec{p}_D - \vec{p}_{b_1} - \vec{p}_{e^+}, \tag{4}$$

where $E_{b_1(e^+)}$ and $\vec{p}_{b_1(e^+)}$ are the measured energy and momentum of the b_1 (e^+) candidate in the e^+e^- center-of-mass frame, respectively. We calculate $\vec{p}_D \equiv -\hat{p}_{\bar{D}}\sqrt{E^2_{\rm beam}/c^2 - m^2_{\bar{D}} \cdot c^2}$, where $\hat{p}_{\bar{D}}$ is a unit vector in the momentum direction of the ST $\bar{D}$ meson and $m_{\bar{D}}$ is the known $\bar{D}$ mass [3]. The beam energy and the known D mass are used to determine the magnitude of the momentum of the ST D meson in order to improve the $U_{\rm miss}$ resolution. The signal candidates are expected to peak around zero in the $U_{\rm miss}$ distribution and near the invariant mass of the b_1 in the $\omega\pi$ mass spectrum ($M_{\omega\pi}$).

To obtain the signal yields, we perform two-dimensional (2D) unbinned maximum likelihood fits to the $M_{\omega\pi^{-(0)}}$ versus $U_{\rm miss}$ distributions. In the fits, the 2D signal and background shapes are modeled by the simulated shapes derived from the signal and inclusive MC samples, respectively, and the yields of the signal and background are left free. The projections of the 2D fit on the $M_{\omega\pi^{-(0)}}$ and $U_{\rm miss}$ distributions are shown in Fig. 2. From the fits, the signal yields are $N_{\rm DT} = 35.6 \pm 8.9$ and $N_{\rm DT} = 17.5 \pm 6.7$ for $D^0 \to b_1^- e^+ \nu_e$ and $D^+ \to b_1^0 e^+ \nu_e$, respectively, and the signal significances are estimated to be 5.2σ and 3.1σ, by comparing the likelihoods with or without the signal

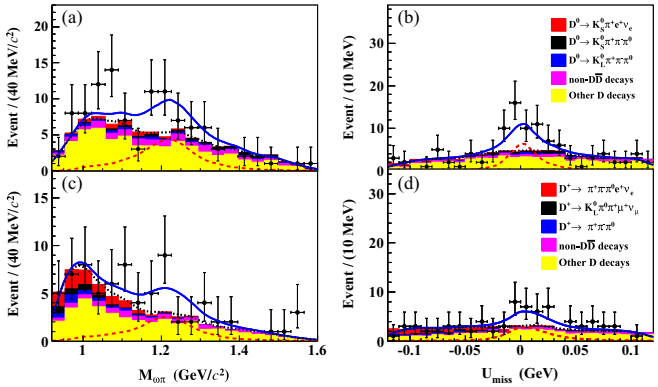

FIG. 2. The projections onto (a),(c) $M_{\omega\pi^{-(0)}}$ and (b),(d) $U_{\rm miss}$ for the decays (a),(b) $D^0 \to b_1^- e^+ \nu_e$ and (c),(d) $D^+ \to b_1^0 e^+ \nu_e$. The dots with error bars are data. The blue solid, red dashed, and black dashed curves are the fit results, the fitted signals, and the fitted backgrounds, respectively. The color-filled histograms are from different background sources, as labeled in the legend.

involved and taking into account the change of degrees of freedom. Because the nonresonant component is highly suppressed in semileptonic D decays and due to limited statistics, all $\omega\pi$ candidates are assumed to come from b_1 decays. The nonresonant component is considered as a source of systematic uncertainty. Based on MC simulations, the detection efficiencies $\bar{\varepsilon}_{\rm SL}$ are estimated to be 0.0715 ± 0.0005 and 0.0417 ± 0.0004 for $D^0 \to b_1^- e^+ \nu_e$ and $D^+ \to b_1^0 e^+ \nu_e$, respectively.

The systematic uncertainties in the branching fraction measurements are discussed below. The uncertainty associated with the ST yield $N^{\rm tot}_{\rm ST}$ is estimated to be 0.3% [48]. The uncertainty from the quoted branching fraction of $\omega \to \pi^+\pi^-\pi^0$ is 0.8% [3]. The efficiencies of the e^+ tracking and PID are investigated using a control sample of $e^+e^- \to \gamma e^+ e^-$ [48], and those of the $\pi^\pm$ tracking and PID as well as for π^0 reconstruction are estimated with control samples of $D^0 \to K^-\pi^+$, $D^0 \to K^-\pi^+\pi^0$, $D^0 \to K^-\pi^+\pi^+\pi^-$, and $D^+ \to K^-\pi^+\pi^+$ with the same tags. The systematic uncertainties in the tracking (PID) are assigned as 1.0% (1.0%) per e^+ and 1.0% (1.0%) per $\pi^\pm$, respectively. The systematic uncertainty of the π^0 reconstruction, including photon finding, the π^0 mass window, and the 1C kinematic fit, is assigned as 2.0% per π^0 [49].

The systematic uncertainty associated with the ω mass window is assigned to be 1.9% using a control sample of $D^0 \to K^0_S\omega$ reconstructed versus the same $\bar{D}^0$ tags as the nominal analysis. The systematic uncertainties arising from the $E^{\rm max}_{{\rm extra}\,\gamma}$ and $N_{{\rm extra},\pi^0}$ requirements are estimated to be 1.8% and 2.0% for $D^0 \to b_1^- e^+ \nu_e$ and $D^+ \to b_1^0 e^+ \nu_e$, respectively, which are estimated using the DT samples of $D^0 \to K^- e^+ \nu_e$ and $D^+ \to K^0_S e^+ \nu_e$ decays reconstructed versus the same tags as the nominal analysis. The systematic uncertainty related to the b_1 resonant parameters is estimated using alternative signal MC samples, which are

produced by varying the mass and width of the b_1 by $\pm 1\sigma$. The maximum changes of the signal efficiencies, 1.4% and 4.8%, are assigned as the systematic uncertainties for $D^0 \to b_1^- e^+ \nu_e$ and $D^+ \to b_1^0 e^+ \nu_e$, respectively. The uncertainty from limited MC statistics is estimated to be 0.3%. The systematic uncertainty due to the MC generator is assigned by examining the DT efficiency with the signal MC events produced with the phase space model. The maximum changes of the DT efficiencies, 1.4% and 0.5%, are assigned as the systematic uncertainties for $D^0 \to b_1^- e^+ \nu_e$ and $D^+ \to b_1^0 e^+ \nu_e$, respectively. The systematic uncertainty associated with the $\cos\theta_{\gamma,\mathrm{miss}}$ requirement is estimated to be 1.0% by analyzing the DT sample of $D^0 \to K_S^0 \pi^- e^+ \nu_e$. The systematic uncertainty due to the sideband estimation of the ω background, which may be from $D^{0(+)} \to b_1^{-(0)} e^+ \nu_e$ with $b_1^{-(0)} \to \pi^+\pi^-\pi^0\pi^{0(-)}$, is estimated by examining the measured branching fractions after considering this contribution. The changes in the branching fractions, 0.5% and 4.6%, are taken as the corresponding systematic uncertainties.

To estimate the systematic uncertainties of the signal and background shapes in the U_{miss} fit, a simulated shape convolved with a double Gaussian function with floating parameters is chosen as the alternative signal shape, and the simulated background shape derived from the inclusive MC sample is replaced with a first-order Chebyshev polynomial function. The differences in the fitted signal yields are taken as individual systematic uncertainties. The uncertainty arising from the background shape is mainly due to unknown nonresonant decays and is assigned as the change of the fitted DT yield when they are fixed by referring to the well-known nonresonant fraction in $D^+ \to \bar{K}^*(892)^0 e^+ \nu_e$ [50]. The total systematic uncertainties are $^{+8.8\%}_{-10.7\%}$ and $^{+12.7\%}_{-13.9\%}$ by adding all the individual contributions in quadrature for $D^0 \to b_1^- e^+ \nu_e$ and $D^+ \to b_1^0 e^+ \nu_e$, respectively.

The product branching fractions are determined to be $\mathcal{B}(D^0 \to b_1^- e^+ \nu_e) \times \mathcal{B}(b^- \to \omega\pi^-) = (0.72 \pm 0.18^{+0.06}_{-0.08}) \times 10^{-4}$ and $\mathcal{B}(D^+ \to b_1^0 e^+ \nu_e) \times \mathcal{B}(b_1^0 \to \omega\pi^0) = (1.16 \pm 0.44 \pm 0.16) \times 10^{-4}$ for $D^0 \to b_1^- e^+ \nu_e$ and $D^+ \to b_1^0 e^+ \nu_e$, where the first and second uncertainties are statistical and systematic, respectively.

In summary, by analyzing 7.9 fb^{-1} of e^+e^- collision data taken at $\sqrt{s} = 3.773$ GeV, we report the first observation of $D^0 \to b_1^- e^+ \nu_e$ with a significance of 5.2σ and find the first evidence for $D^+ \to b_1^0 e^+ \nu_e$ with a significance of 3.1σ after considering systematic uncertainty. Their product branching fractions are determined to be $\mathcal{B}(D^0 \to b_1^- e^+ \nu_e) \times \mathcal{B}(b_1^- \to \omega\pi^-) = (0.72 \pm 0.18^{+0.06}_{-0.08}) \times 10^{-4}$ and $\mathcal{B}(D^+ \to b_1^0 e^+ \nu_e) \times \mathcal{B}(b_1^0 \to \omega\pi^0) = (1.16 \pm 0.44 \pm 0.16) \times 10^{-4}$. Assuming $\mathcal{B}(b_1 \to \omega\pi) = 1$, these results are comparable with the theoretical predictions reported in Refs. [2,6], thereby implying that the $\omega\pi$ final state is currently the dominant decay mode of b_1, which aligns with the leading-order predictions of Refs. [23–25], but conflicts with the NLO calculations from Ref. [23]. Using the obtained branching fractions, the world-average lifetimes of the D^0 and D^+ mesons [3], and assuming that $\mathcal{B}(b_1^- \to \omega\pi^-) = \mathcal{B}(b_1^0 \to \omega\pi^0)$, we determine the partial decay width ratio $[\Gamma(D^0 \to b_1^- e^+ \nu_e)/2\Gamma(D^+ \to b_1^0 e^+ \nu_e)] = 0.78 \pm 0.19^{+0.04}_{-0.05}$, which is consistent with unity within uncertainties after considering the shared systematic terms and is thus consistent with isospin conservation. Observation of the b_1 in semileptonic D decays opens a new avenue for experimental investigation. Future analysis of their decay dynamics, which will be made possible with the larger data sample at BESIII [26] and a potential future STCF [51], will provide deep insights into the inner structure, production, mass, and width of the b_1, as well as provide access to hadronic-transition form factors, and strong phase, which sheds light on the phase of elastic $\omega\pi$ scattering.

Acknowledgments—The authors appreciate Lisheng Geng, Qiang Zhao, and Feng-Kun Guo for useful discussions. The BESIII Collaboration thanks the staff of BEPCII and the IHEP computing center for their strong support. This work is supported in part by National Key R&D Program of China under Contracts No. 2023YFA1606000, No. 2023YFA1606704, No. 2020YFA0406300, and No. 2020YFA0406400; National Natural Science Foundation of China (NSFC) under Contracts No. 12375092, No. 11635010, No. 11735014, No. 11935015, No. 11935016, No. 11935018, No. 11961141012, No. 12025502, No. 12035009, No. 12035013, No. 12061131003, No. 12192260, No. 12192261, No. 12192262, No. 12192263, No. 12192264, No. 12192265, No. 12221005, No. 12225509, and No. 12235017; the Chinese Academy of Sciences (CAS) Large-Scale Scientific Facility Program; the CAS Center for Excellence in Particle Physics (CCEPP); Joint Large-Scale Scientific Facility Funds of the NSFC and CAS under Contract No. U1832207; 100 Talents Program of CAS; The Institute of Nuclear and Particle Physics (INPAC) and Shanghai Key Laboratory for Particle Physics and Cosmology; German Research Foundation DFG under Contracts No. 455635585, No. FOR5327, and No. GRK 2149; Istituto Nazionale di Fisica Nucleare, Italy; Ministry of Development of Turkey under Contract No. DPT2006K-120470; National Research Foundation of Korea under Contract No. NRF-2022R1A2C1092335; National Science and Technology fund of Mongolia; National Science Research and Innovation Fund (NSRF) via the Program Management Unit for Human Resources and Institutional Development, Research and Innovation of Thailand under Contract No. B16F640076; Polish National Science Centre under Contract No. 2019/35/O/ST2/02907; the Swedish Research Council; U.S. Department of Energy under Contract No. DE-FG02-05ER41374.

[1] N. Isgur, D. Scora, B. Grinstein, and M. B. Wise, Phys. Rev. D **39**, 799 (1989).
[2] D. Scora and N. Isgur, Phys. Rev. D **52**, 2783 (1995).
[3] S. Navas *et al.* (Particle Data Group), Phys. Rev. D **110**, 030001 (2024).
[4] B. C. Ke, J. Koponen, H. B. Li, and Y. Zheng, Annu. Rev. Nucl. Part. Sci. **73**, 285 (2023).
[5] H. B. Li and X. R. Lyu, Natl. Sci. Rev. **8**, nwab181 (2021).
[6] H. Y. Cheng and X. W. Kang, Eur. Phys. J. C **77**, 587 (2017); **77**, 863(E) (2017).
[7] M. A. Abolins, R. L. Lander, W. A. W. Mehlhop, N. huu Xuong, and P. M. Yager, Phys. Rev. Lett. **11**, 381 (1963).
[8] R. Bizzarri, M. Foster, P. Gavillet, G. Labrosse, L. Montanet, R. Salmeron, P. Villemoes, C. Ghesquiere, and E. Lillestol, Nucl. Phys. **B14**, 169 (1969).
[9] C. Baltay, J. C. Severiens, N. Yeh, and D. Zanello, Phys. Rev. Lett. **18**, 93 (1967).
[10] M. Atkinson *et al.* (Omega Photon Collaboration), Phys. Lett. **138B**, 459 (1984).
[11] U. Karshon, G. Mikenberg, Y. Eisenberg, S. Pitluck, E. E. Ronat, A. Shapira, and G. Yekutieli, Phys. Rev. D **10**, 3608 (1974).
[12] V. Chaloupka, A. Ferrando, M. J. Losty, and L. Montanet, Phys. Lett. **51B**, 407 (1974).
[13] R. Gessaroli *et al.*, Nucl. Phys. **B126**, 382 (1977).
[14] C. Evangelista *et al.*, Nucl. Phys. **B178**, 197 (1981); **B186**, 594(E) (1981); **A435**, 859(E) (1985).
[15] M. Atkinson *et al.* (Omega Photon Collaboration), Nucl. Phys. **B243**, 1 (1984).
[16] B. Collick *et al.*, Phys. Rev. Lett. **53**, 2374 (1984).
[17] S. Fukui *et al.*, Phys. Lett. B **257**, 241 (1991).
[18] A. Alde *et al.* (IHEP-IISN-LANL-LAPP-KEK Collaboration), Z. Phys. C **54**, 553 (1992).
[19] P. Weidenauer *et al.* (ASTERIX Collaboration), Z. Phys. C **54**, 553 (1992).
[20] S. Ishida, M. Oda, H. Sawazaki, and K. Yamada, Prog. Theor. Phys. **88**, 89 (1992).
[21] M. F. M. Lutz and E. E. Kolomeitsev, Nucl. Phys. **A730**, 392 (2004).
[22] L. Roca, E. Oset, and J. Singh, Phys. Rev. D **72**, 014002 (2005).
[23] Y. Zhou, X. L. Ren, H. X. Chen, and L. S. Geng, Phys. Rev. D **90**, 014020 (2014).
[24] W. H. Liang, S. Sakai, and E. Oset, Phys. Rev. D **99**, 094020 (2019).
[25] S. Clymton and H. C. Kim, Phys. Rev. D **108**, 074021 (2023).
[26] M. Ablikim *et al.* (BESIII Collaboration), Chin. Phys. C **44**, 040001 (2020).
[27] M. A. Ivanov, J. G. Körner, J. N. Pandya, P. Santorelli, N. R. Soni, and C.-T. Tran, Front. Phys. **14**, 644016 (2019).
[28] L. R. Dai, L. Roca, and E. Oset, Eur. Phys. J. C **80**, 673 (2020).
[29] L. R. Dai, L. Roca, and E. Oset, Phys. Rev. D **99**, 096003 (2019).
[30] H. Y. Jing, X. Liu, and Z. J. Xiao, Phys. Rev. D **96**, 113002 (2017).
[31] Z. Q. Zhang, arXiv:1203.5913.
[32] Z. Q. Zhang, Phys. Rev. D **85**, 114005 (2012).
[33] S. Momeni and R. Khosravi, J. Phys. G **46**, 105006 (2019).
[34] S. Momeni and M. Saghebfar, Eur. Phys. J. C **82**, 473 (2022).
[35] U. G. Meißner and J. A. Oller, Nucl. Phys. **A679**, 671 (2001).
[36] L. Roca, J. E. Palomar, E. Oset, and H. C. Chiang, Nucl. Phys. **A744**, 127 (2004).
[37] W. H. Liang, S. Sakai, and E. Oset, Phys. Rev. D **99**, 094020 (2019).
[38] M. Ablikim *et al.* (BESIII Collaboration), Phys. Rev. D **102**, 112005 (2020).
[39] M. Ablikim *et al.* (BESIII Collaboration), Chin. Phys. C **48**, 123001 (2024).
[40] M. Ablikim *et al.* (BESIII Collaboration), Nucl. Instrum. Methods Phys. Res., Sect. A **614**, 345 (2010).
[41] X. Li *et al.*, Radiat. Detect. Technol. Methods **1**, 13 (2017); Y. X. Guo *et al.*, Radiat. Detect. Technol. Methods **1**, 15 (2017); P. Cao *et al.*, Nucl. Instrum. Methods Phys. Res., Sect. A **953**, 163053 (2020).
[42] S. Agostinelli *et al.* (Geant4 Collaboration), Nucl. Instrum. Methods Phys. Res., Sect. A **506**, 250 (2003).
[43] S. Jadach, B. F. L. Ward, and Z. Was, Comput. Phys. Commun. **130**, 260 (2000); Phys. Rev. D **63**, 113009 (2001).
[44] D. J. Lange, Nucl. Instrum. Methods Phys. Res., Sect. A **462**, 152 (2001); R. G. Ping, Chin. Phys. C **32**, 599 (2008).
[45] J. C. Chen, G. S. Huang, X. R. Qi, D. H. Zhang, and Y. S. Zhu, Phys. Rev. D **62**, 034003 (2000).
[46] E. Richter-Was, Phys. Lett. B **303**, 163 (1993).
[47] H. Albrecht *et al.* (ARGUS Collaboration), Phys. Lett. B **241**, 278 (1990).
[48] M. Ablikim *et al.* (BESIII Collaboration), Phys. Rev. D **109**, 072003 (2024).
[49] M. Ablikim *et al.* (BESIII Collaboration), Phys. Rev. D **83**, 112005 (2011).
[50] M. Ablikim *et al.* (BESIII Collaboration), Phys. Rev. D **94**, 032001 (2016).
[51] M. Achasov *et al.*, Front. Phys. **19**, 14701 (2024).

M. Ablikim,[1] M. N. Achasov,[4,c] P. Adlarson,[76] O. Afedulidis,[3] X. C. Ai,[81] R. Aliberti,[35] A. Amoroso,[75a,75c] Q. An,[58,72,a] Y. Bai,[57] O. Bakina,[36] I. Balossino,[29a] Y. Ban,[46,h] H.-R. Bao,[64] V. Batozskaya,[1,44] K. Begzsuren,[32] N. Berger,[35] M. Berlowski,[44] M. Bertani,[28a] D. Bettoni,[29a] F. Bianchi,[75a,75c] E. Bianco,[75a,75c] A. Bortone,[75a,75c] I. Boyko,[36] R. A. Briere,[5] A. Brueggemann,[69] H. Cai,[77] X. Cai,[1,58] A. Calcaterra,[28a] G. F. Cao,[1,64] N. Cao,[1,64] S. A. Cetin,[62a] X. Y. Chai,[46,h] J. F. Chang,[1,58] G. R. Che,[43] Y. Z. Che,[1,58,64] G. Chelkov,[36,b] C. Chen,[43] C. H. Chen,[9] Chao Chen,[55] G. Chen,[1] H. S. Chen,[1,64] H. Y. Chen,[20] M. L. Chen,[1,58,64] S. J. Chen,[42] S. L. Chen,[45] S. M. Chen,[61] T. Chen,[1,64] X. R. Chen,[31,64] X. T. Chen,[1,64]

Y. B. Chen,[1,58] Y. Q. Chen,[34] Z. J. Chen,[25,i] Z. Y. Chen,[1,64] S. K. Choi,[10] G. Cibinetto,[29a] F. Cossio,[75c] J. J. Cui,[50] H. L. Dai,[1,58] J. P. Dai,[79] A. Dbeyssi,[18] R. E. de Boer,[3] D. Dedovich,[36] C. Q. Deng,[73] Z. Y. Deng,[1] A. Denig,[35] I. Denysenko,[36] M. Destefanis,[75a,75c] F. De Mori,[75a,75c] B. Ding,[1,67] X. X. Ding,[46,h] Y. Ding,[40] Y. Ding,[34] J. Dong,[1,58] L. Y. Dong,[1,64] M. Y. Dong,[1,58,64] X. Dong,[77] M. C. Du,[1] S. X. Du,[81] Y. Y. Duan,[55] Z. H. Duan,[42] P. Egorov,[36,b] Y. H. Fan,[45] J. Fang,[1,58] J. Fang,[59] S. S. Fang,[1,64] W. X. Fang,[1] Y. Fang,[1] Y. Q. Fang,[1,58] R. Farinelli,[29a] L. Fava,[75b,75c] F. Feldbauer,[3] G. Felici,[28a] C. Q. Feng,[58,72] J. H. Feng,[59] Y. T. Feng,[58,72] M. Fritsch,[3] C. D. Fu,[1] J. L. Fu,[64] Y. W. Fu,[1,64] H. Gao,[64] X. B. Gao,[41] Y. N. Gao,[46,h] Yang Gao,[58,72] S. Garbolino,[75c] I. Garzia,[29a,29b] L. Ge,[81] P. T. Ge,[19] Z. W. Ge,[42] C. Geng,[59] E. M. Gersabeck,[68] A. Gilman,[70] K. Goetzen,[13] L. Gong,[40] W. X. Gong,[1,58] W. Gradl,[35] S. Gramigna,[29a,29b] M. Greco,[75a,75c] M. H. Gu,[1,58] Y. T. Gu,[15] C. Y. Guan,[1,64] A. Q. Guo,[31,64] L. B. Guo,[41] M. J. Guo,[50] R. P. Guo,[49] Y. P. Guo,[12,g] A. Guskov,[36,b] J. Gutierrez,[27] K. L. Han,[64] T. T. Han,[1] F. Hanisch,[3] X. Q. Hao,[19] F. A. Harris,[66] K. K. He,[55] K. L. He,[1,64] F. H. Heinsius,[3] C. H. Heinz,[35] Y. K. Heng,[1,58,64] C. Herold,[60] T. Holtmann,[3] P. C. Hong,[34] G. Y. Hou,[1,64] X. T. Hou,[1,64] Y. R. Hou,[64] Z. L. Hou,[1] B. Y. Hu,[59] H. M. Hu,[1,64] J. F. Hu,[56,j] S. L. Hu,[12,g] T. Hu,[1,58,64] Y. Hu,[1] G. S. Huang,[58,72] K. X. Huang,[59] L. Q. Huang,[31,64] X. T. Huang,[50] Y. P. Huang,[1] Y. S. Huang,[59] T. Hussain,[74] F. Hölzken,[3] N. Hüsken,[35] N. in der Wiesche,[69] J. Jackson,[27] S. Janchiv,[32] J. H. Jeong,[10] Q. Ji,[1] Q. P. Ji,[19] W. Ji,[1,64] X. B. Ji,[1,64] X. L. Ji,[1,58] Y. Y. Ji,[50] X. Q. Jia,[50] Z. K. Jia,[58,72] D. Jiang,[1,64] H. B. Jiang,[77] P. C. Jiang,[46,h] S. S. Jiang,[39] T. J. Jiang,[16] X. S. Jiang,[1,58,64] Y. Jiang,[64] J. B. Jiao,[50] J. K. Jiao,[34] Z. Jiao,[23] S. Jin,[42] Y. Jin,[67] M. Q. Jing,[1,64] X. M. Jing,[64] T. Johansson,[76] S. Kabana,[33] N. Kalantar-Nayestanaki,[65] X. L. Kang,[9] X. S. Kang,[40] M. Kavatsyuk,[65] B. C. Ke,[81] V. Khachatryan,[27] A. Khoukaz,[69] R. Kiuchi,[1] O. B. Kolcu,[62a] B. Kopf,[3] M. Kuessner,[3] X. Kui,[1,64] N. Kumar,[26] A. Kupsc,[44,76] W. Kühn,[37] J. J. Lane,[68] L. Lavezzi,[75a,75c] T. T. Lei,[58,72] Z. H. Lei,[58,72] M. Lellmann,[35] T. Lenz,[35] C. Li,[47] C. Li,[43] C. H. Li,[39] Cheng Li,[58,72] D. M. Li,[81] F. Li,[1,58] G. Li,[1] H. B. Li,[1,64] H. J. Li,[19] H. N. Li,[56,j] Hui Li,[43] J. R. Li,[61] J. S. Li,[59] K. Li,[1] K. L. Li,[19] L. J. Li,[1,64] L. K. Li,[1] Lei Li,[48] M. H. Li,[43] P. R. Li,[38,k,l] Q. M. Li,[1,64] Q. X. Li,[50] R. Li,[17,31] S. X. Li,[12] T. Li,[50] W. D. Li,[1,64] W. G. Li,[1,a] X. Li,[1,64] X. H. Li,[58,72] X. L. Li,[50] X. Y. Li,[1,64] X. Z. Li,[59] Y. G. Li,[46,h] Z. J. Li,[59] Z. Y. Li,[79] C. Liang,[42] H. Liang,[58,72] Hao Liang,[1,64] Y. F. Liang,[54] Y. T. Liang,[31,64] G. R. Liao,[14] Y. P. Liao,[1,64] J. Libby,[26] A. Limphirat,[60] C. C. Lin,[55] D. X. Lin,[31,64] T. Lin,[1] B. J. Liu,[1] B. X. Liu,[77] C. Liu,[34] C. X. Liu,[1] F. Liu,[1] F. H. Liu,[53] Feng Liu,[6] G. M. Liu,[56,j] H. Liu,[38,k,l] H. B. Liu,[15] H. H. Liu,[1] H. M. Liu,[1,64] Huihui Liu,[21] J. B. Liu,[58,72] J. Y. Liu,[1,64] K. Liu,[38,k,l] K. Y. Liu,[40] Ke Liu,[22] L. Liu,[58,72] L. C. Liu,[43] Lu Liu,[43] M. H. Liu,[12,g] P. L. Liu,[1] Q. Liu,[64] S. B. Liu,[58,72] T. Liu,[12,g] W. K. Liu,[43] W. M. Liu,[58,72] X. Liu,[38,k,l] X. Liu,[39] Y. Liu,[38,k,l] Y. Liu,[81] Y. B. Liu,[43] Z. A. Liu,[1,58,64] Z. D. Liu,[9] Z. Q. Liu,[50] X. C. Lou,[1,58,64] F. X. Lu,[59] H. J. Lu,[23] J. G. Lu,[1,58] X. L. Lu,[1] Y. Lu,[7] Y. P. Lu,[1,58] Z. H. Lu,[1,64] C. L. Luo,[41] J. R. Luo,[59] M. X. Luo,[80] T. Luo,[12,g] X. L. Luo,[1,58] X. R. Lyu,[64] Y. F. Lyu,[43] F. C. Ma,[40] H. Ma,[79] H. L. Ma,[1] J. L. Ma,[1,64] L. L. Ma,[50] L. R. Ma,[67] M. M. Ma,[1,64] Q. M. Ma,[1] R. Q. Ma,[1,64] T. Ma,[58,72] X. T. Ma,[1,64] X. Y. Ma,[1,58] Y. M. Ma,[31] F. E. Maas,[18] I. MacKay,[70] M. Maggiora,[75a,75c] S. Malde,[70] Y. J. Mao,[46,h] Z. P. Mao,[1] S. Marcello,[75a,75c] Z. X. Meng,[67] J. G. Messchendorp,[13,65] G. Mezzadri,[29a] H. Miao,[1,64] T. J. Min,[42] R. E. Mitchell,[27] X. H. Mo,[1,58,64] B. Moses,[27] N. Yu. Muchnoi,[4,c] J. Muskalla,[35] Y. Nefedov,[36] F. Nerling,[18,e] L. S. Nie,[20] I. B. Nikolaev,[4,c] Z. Ning,[1,58] S. Nisar,[11,m] Q. L. Niu,[38,k,l] W. D. Niu,[55] Y. Niu,[50] S. L. Olsen,[10,64] Q. Ouyang,[1,58,64] S. Pacetti,[28b,28c] X. Pan,[55] Y. Pan,[57] A. Pathak,[34] Y. P. Pei,[58,72] M. Pelizaeus,[3] H. P. Peng,[58,72] Y. Y. Peng,[38,k,l] K. Peters,[13,e] J. L. Ping,[41] R. G. Ping,[1,64] S. Plura,[35] V. Prasad,[33] F. Z. Qi,[1] H. Qi,[58,72] H. R. Qi,[61] M. Qi,[42] T. Y. Qi,[12,g] S. Qian,[1,58] W. B. Qian,[64] C. F. Qiao,[64] X. K. Qiao,[81] J. J. Qin,[73] L. Q. Qin,[14] L. Y. Qin,[58,72] X. P. Qin,[12,g] X. S. Qin,[50] Z. H. Qin,[1,58] J. F. Qiu,[1] Z. H. Qu,[73] K. Ravindran,[82] C. F. Redmer,[35] K. J. Ren,[39] A. Rivetti,[75c] M. Rolo,[75c] G. Rong,[1,64] Ch. Rosner,[18] M. Q. Ruan,[1,58] S. N. Ruan,[43] N. Salone,[44] A. Sarantsev,[36,d] Y. Schelhaas,[35] K. Schoenning,[76] M. Scodeggio,[29a] K. Y. Shan,[12,g] W. Shan,[24] X. Y. Shan,[58,72] Z. J. Shang,[38,k,l] J. F. Shangguan,[16] L. G. Shao,[1,64] M. Shao,[58,72] C. P. Shen,[12,g] H. F. Shen,[1,8] W. H. Shen,[64] X. Y. Shen,[1,64] B. A. Shi,[64] H. Shi,[58,72] H. C. Shi,[58,72] J. L. Shi,[12,g] J. Y. Shi,[1] Q. Q. Shi,[55] S. Y. Shi,[73] X. Shi,[1,58] J. J. Song,[19] T. Z. Song,[59] W. M. Song,[1,34] Y. J. Song,[12,g] Y. X. Song,[46,h,n] S. Sosio,[75a,75c] S. Spataro,[75a,75c] F. Stieler,[35] S. S. Su,[40] Y. J. Su,[64] G. B. Sun,[77] G. X. Sun,[1] H. Sun,[64] H. K. Sun,[1] J. F. Sun,[19] K. Sun,[61] L. Sun,[77] S. S. Sun,[1,64] T. Sun,[51,f] W. Y. Sun,[34] Y. Sun,[9] Y. J. Sun,[58,72] Y. Z. Sun,[1] Z. Q. Sun,[1,64] Z. T. Sun,[50] C. J. Tang,[54] G. Y. Tang,[1] J. Tang,[59] M. Tang,[58,72] Y. A. Tang,[77] L. Y. Tao,[73] Q. T. Tao,[25,i] M. Tat,[70] J. X. Teng,[58,72] V. Thoren,[76] W. H. Tian,[59] Y. Tian,[31,64] Z. F. Tian,[77] I. Uman,[62b] Y. Wan,[55] S. J. Wang,[50] B. Wang,[1] B. L. Wang,[64] Bo Wang,[58,72] D. Y. Wang,[46,h] F. Wang,[73] H. J. Wang,[38,k,l] J. J. Wang,[77] J. P. Wang,[50] K. Wang,[1,58] L. L. Wang,[1] M. Wang,[50] N. Y. Wang,[64] S. Wang,[12,g] S. Wang,[38,k,l] T. Wang,[12,g] T. J. Wang,[43] W. Wang,[59] Wei Wang,[73] W. P. Wang,[35,58,72,o] X. Wang,[46,h] X. F. Wang,[38,k,l] X. J. Wang,[39] X. L. Wang,[12,g] X. N. Wang,[1] Y. Wang,[61] Y. D. Wang,[45] Y. F. Wang,[1,58,64] Y. L. Wang,[19] Y. N. Wang,[45] Y. Q. Wang,[1] Yaqian Wang,[17] Yi Wang,[61] Z. Wang,[1,58] Z. L. Wang,[73] Z. Y. Wang,[1,64] Ziyi Wang,[64] D. H. Wei,[14] F. Weidner,[69] S. P. Wen,[1] Y. R. Wen,[39] U. Wiedner,[3] G. Wilkinson,[70]

M. Wolke,[76] L. Wollenberg,[3] C. Wu,[39] J. F. Wu,[1,8] L. H. Wu,[1] L. J. Wu,[1,64] X. Wu,[73,12,g] X. H. Wu,[34] Y. Wu,[58,72] Y. H. Wu,[55] Y. J. Wu,[31] Z. Wu,[1,58] L. Xia,[58,72] X. M. Xian,[39] B. H. Xiang,[1,64] T. Xiang,[46,h] D. Xiao,[38,k,l] G. Y. Xiao,[42] S. Y. Xiao,[1] Y. L. Xiao,[12,g] Z. J. Xiao,[41] C. Xie,[42] X. H. Xie,[46,h] Y. Xie,[50] Y. G. Xie,[1,58] Y. H. Xie,[6] Z. P. Xie,[58,72] T. Y. Xing,[1,64] C. F. Xu,[1,64] C. J. Xu,[59] G. F. Xu,[1] H. Y. Xu,[2,67,p] M. Xu,[58,72] Q. J. Xu,[16] Q. N. Xu,[30] W. Xu,[1] W. L. Xu,[67] X. P. Xu,[55] Y. Xu,[40] Y. C. Xu,[78] Z. S. Xu,[64] F. Yan,[12,g] L. Yan,[12,g] W. B. Yan,[58,72] W. C. Yan,[81] X. Q. Yan,[1,64] H. J. Yang,[51,f] H. L. Yang,[34] H. X. Yang,[1] J. H. Yang,[42] T. Yang,[1] Y. Yang,[12,g] Y. F. Yang,[1,64] Y. F. Yang,[43] Y. X. Yang,[1,64] Z. W. Yang,[38,k,l] Z. P. Yao,[50] M. Ye,[1,58] M. H. Ye,[8] J. H. Yin,[1] Junhao Yin,[43] Z. Y. You,[59] B. X. Yu,[1,58,64] C. X. Yu,[43] G. Yu,[1,64] J. S. Yu,[25,i] M. C. Yu,[40] T. Yu,[73] X. D. Yu,[46,h] Y. C. Yu,[81] C. Z. Yuan,[1,64] J. Yuan,[34] J. Yuan,[45] L. Yuan,[2] S. C. Yuan,[1,64] Y. Yuan,[1,64] Z. Y. Yuan,[59] C. X. Yue,[39] A. A. Zafar,[74] F. R. Zeng,[50] S. H. Zeng,[63] X. Zeng,[12,g] Y. Zeng,[25,i] Yujie Zeng,[59] Y. J. Zeng,[1,64] X. Y. Zhai,[34] Y. C. Zhai,[50] Y. H. Zhan,[59] A. Q. Zhang,[1,64] B. L. Zhang,[1,64] B. X. Zhang,[1] D. H. Zhang,[43] G. Y. Zhang,[19] H. Zhang,[58,72] H. Zhang,[81] H. C. Zhang,[1,58,64] H. H. Zhang,[59] H. H. Zhang,[34] H. Q. Zhang,[1,58,64] H. R. Zhang,[58,72] H. Y. Zhang,[1,58] Jin Zhang,[81] J. Zhang,[59] J. J. Zhang,[52] J. L. Zhang,[20] J. Q. Zhang,[41] J. S. Zhang,[12,g] J. W. Zhang,[1,58,64] J. X. Zhang,[38,k,l] J. Y. Zhang,[1] J. Z. Zhang,[1,64] Jianyu Zhang,[64] L. M. Zhang,[61] Lei Zhang,[42] P. Zhang,[1,64] Q. Y. Zhang,[34] R. Y. Zhang,[38,k,l] S. H. Zhang,[1,64] Shulei Zhang,[25,i] X. M. Zhang,[1] X. Y. Zhang,[40] X. Y. Zhang,[50] Y. Zhang,[1] Y. Zhang,[73] Y. T. Zhang,[81] Y. H. Zhang,[1,58] Y. M. Zhang,[39] Yan Zhang,[58,72] Z. D. Zhang,[1] Z. H. Zhang,[1] Z. L. Zhang,[34] Z. Y. Zhang,[77] Z. Y. Zhang,[43] Z. Z. Zhang,[45] G. Zhao,[1] J. Y. Zhao,[1,64] J. Z. Zhao,[1,58] L. Zhao,[1] Lei Zhao,[58,72] M. G. Zhao,[43] N. Zhao,[79] R. P. Zhao,[64] S. J. Zhao,[81] Y. B. Zhao,[1,58] Y. X. Zhao,[31,64] Z. G. Zhao,[58,72] A. Zhemchugov,[36,b] B. Zheng,[73] B. M. Zheng,[34] J. P. Zheng,[1,58] W. J. Zheng,[1,64] Y. H. Zheng,[64] B. Zhong,[41] X. Zhong,[59] H. Zhou,[50] J. Y. Zhou,[34] L. P. Zhou,[1,64] S. Zhou,[6] X. Zhou,[77] X. K. Zhou,[6] X. R. Zhou,[58,72] X. Y. Zhou,[39] Y. Z. Zhou,[12,g] Z. C. Zhou,[20] A. N. Zhu,[64] J. Zhu,[43] K. Zhu,[1] K. J. Zhu,[1,58,64] K. S. Zhu,[12,g] L. Zhu,[34] L. X. Zhu,[64] S. H. Zhu,[71] T. J. Zhu,[12,g] W. D. Zhu,[41] Y. C. Zhu,[58,72] Z. A. Zhu,[1,64] J. H. Zou,[1] and J. Zu[58,72]

(BESIII Collaboration)

[1]*Institute of High Energy Physics, Beijing 100049, People's Republic of China*
[2]*Beihang University, Beijing 100191, People's Republic of China*
[3]*Bochum Ruhr-University, D-44780 Bochum, Germany*
[4]*Budker Institute of Nuclear Physics SB RAS (BINP), Novosibirsk 630090, Russia*
[5]*Carnegie Mellon University, Pittsburgh, Pennsylvania 15213, USA*
[6]*Central China Normal University, Wuhan 430079, People's Republic of China*
[7]*Central South University, Changsha 410083, People's Republic of China*
[8]*China Center of Advanced Science and Technology, Beijing 100190, People's Republic of China*
[9]*China University of Geosciences, Wuhan 430074, People's Republic of China*
[10]*Chung-Ang University, Seoul, 06974, Republic of Korea*
[11]*COMSATS University Islamabad, Lahore Campus, Defence Road, Off Raiwind Road, 54000 Lahore, Pakistan*
[12]*Fudan University, Shanghai 200433, People's Republic of China*
[13]*GSI Helmholtzcentre for Heavy Ion Research GmbH, D-64291 Darmstadt, Germany*
[14]*Guangxi Normal University, Guilin 541004, People's Republic of China*
[15]*Guangxi University, Nanning 530004, People's Republic of China*
[16]*Hangzhou Normal University, Hangzhou 310036, People's Republic of China*
[17]*Hebei University, Baoding 071002, People's Republic of China*
[18]*Helmholtz Institute Mainz, Staudinger Weg 18, D-55099 Mainz, Germany*
[19]*Henan Normal University, Xinxiang 453007, People's Republic of China*
[20]*Henan University, Kaifeng 475004, People's Republic of China*
[21]*Henan University of Science and Technology, Luoyang 471003, People's Republic of China*
[22]*Henan University of Technology, Zhengzhou 450001, People's Republic of China*
[23]*Huangshan College, Huangshan 245000, People's Republic of China*
[24]*Hunan Normal University, Changsha 410081, People's Republic of China*
[25]*Hunan University, Changsha 410082, People's Republic of China*
[26]*Indian Institute of Technology Madras, Chennai 600036, India*
[27]*Indiana University, Bloomington, Indiana 47405, USA*
[28a]*INFN Laboratori Nazionali di Frascati, INFN Laboratori Nazionali di Frascati, I-00044 Frascati, Italy*
[28b]*INFN Sezione di Perugia, I-06100 Perugia, Italy*
[28c]*University of Perugia, I-06100 Perugia, Italy*

[29a]INFN Sezione di Ferrara, INFN Sezione di Ferrara, I-44122 Ferrara, Italy
[29b]University of Ferrara, I-44122 Ferrara, Italy
[30]Inner Mongolia University, Hohhot 010021, People's Republic of China
[31]Institute of Modern Physics, Lanzhou 730000, People's Republic of China
[32]Institute of Physics and Technology, Peace Avenue 54B, Ulaanbaatar 13330, Mongolia
[33]Instituto de Alta Investigación, Universidad de Tarapacá, Casilla 7D, Arica 1000000, Chile
[34]Jilin University, Changchun 130012, People's Republic of China
[35]Johannes Gutenberg University of Mainz, Johann-Joachim-Becher-Weg 45, D-55099 Mainz, Germany
[36]Joint Institute for Nuclear Research, 141980 Dubna, Moscow region, Russia
[37]Justus-Liebig-Universitaet Giessen, II. Physikalisches Institut, Heinrich-Buff-Ring 16, D-35392 Giessen, Germany
[38]Lanzhou University, Lanzhou 730000, People's Republic of China
[39]Liaoning Normal University, Dalian 116029, People's Republic of China
[40]Liaoning University, Shenyang 110036, People's Republic of China
[41]Nanjing Normal University, Nanjing 210023, People's Republic of China
[42]Nanjing University, Nanjing 210093, People's Republic of China
[43]Nankai University, Tianjin 300071, People's Republic of China
[44]National Centre for Nuclear Research, Warsaw 02-093, Poland
[45]North China Electric Power University, Beijing 102206, People's Republic of China
[46]Peking University, Beijing 100871, People's Republic of China
[47]Qufu Normal University, Qufu 273165, People's Republic of China
[48]Renmin University of China, Beijing 100872, People's Republic of China
[49]Shandong Normal University, Jinan 250014, People's Republic of China
[50]Shandong University, Jinan 250100, People's Republic of China
[51]Shanghai Jiao Tong University, Shanghai 200240, People's Republic of China
[52]Shanxi Normal University, Linfen 041004, People's Republic of China
[53]Shanxi University, Taiyuan 030006, People's Republic of China
[54]Sichuan University, Chengdu 610064, People's Republic of China
[55]Soochow University, Suzhou 215006, People's Republic of China
[56]South China Normal University, Guangzhou 510006, People's Republic of China
[57]Southeast University, Nanjing 211100, People's Republic of China
[58]State Key Laboratory of Particle Detection and Electronics, Beijing 100049, Hefei 230026, People's Republic of China
[59]Sun Yat-Sen University, Guangzhou 510275, People's Republic of China
[60]Suranaree University of Technology, University Avenue 111, Nakhon Ratchasima 30000, Thailand
[61]Tsinghua University, Beijing 100084, People's Republic of China
[62a]Turkish Accelerator Center Particle Factory Group, Istinye University, 34010, Istanbul, Turkey
[62b]Near East University, Nicosia, North Cyprus, 99138, Mersin 10, Turkey
[63]University of Bristol, H H Wills Physics Laboratory, Tyndall Avenue, Bristol BS8 1TL, United Kingdom
[64]University of Chinese Academy of Sciences, Beijing 100049, People's Republic of China
[65]University of Groningen, NL-9747 AA Groningen, The Netherlands
[66]University of Hawaii, Honolulu, Hawaii 96822, USA
[67]University of Jinan, Jinan 250022, People's Republic of China
[68]University of Manchester, Oxford Road, Manchester M13 9PL, United Kingdom
[69]University of Muenster, Wilhelm-Klemm-Strasse 9, 48149 Muenster, Germany
[70]University of Oxford, Keble Road, Oxford OX13RH, United Kingdom
[71]University of Science and Technology Liaoning, Anshan 114051, People's Republic of China
[72]University of Science and Technology of China, Hefei 230026, People's Republic of China
[73]University of South China, Hengyang 421001, People's Republic of China
[74]University of the Punjab, Lahore-54590, Pakistan
[75a]University of Turin and INFN, University of Turin, I-10125, Turin, Italy
[75b]University of Eastern Piedmont, I-15121, Alessandria, Italy
[75c]INFN, I-10125, Turin, Italy
[76]Uppsala University, Box 516, SE-75120 Uppsala, Sweden
[77]Wuhan University, Wuhan 430072, People's Republic of China
[78]Yantai University, Yantai 264005, People's Republic of China
[79]Yunnan University, Kunming 650500, People's Republic of China
[80]Zhejiang University, Hangzhou 310027, People's Republic of China
[81]Zhengzhou University, Zhengzhou 450001, People's Republic of China
[82]University of La Serena, Av. Raúl Bitrán 1305, La Serena, Chile

[a]Deceased.
[b]Also at the Moscow Institute of Physics and Technology, Moscow 141700, Russia.
[c]Also at the Novosibirsk State University, Novosibirsk 630090, Russia.
[d]Also at the NRC "Kurchatov Institute," PNPI, 188300 Gatchina, Russia.
[e]Also at Goethe University Frankfurt, 60323 Frankfurt am Main, Germany.
[f]Also at Key Laboratory for Particle Physics, Astrophysics and Cosmology, Ministry of Education, Shanghai Key Laboratory for Particle Physics and Cosmology, Institute of Nuclear and Particle Physics, Shanghai 200240, People's Republic of China.
[g]Also at Key Laboratory of Nuclear Physics and Ion-beam Application (MOE) and Institute of Modern Physics, Fudan University, Shanghai 200443, People's Republic of China.
[h]Also at State Key Laboratory of Nuclear Physics and Technology, Peking University, Beijing 100871, People's Republic of China.
[i]Also at School of Physics and Electronics, Hunan University, Changsha 410082, China.
[j]Also at Guangdong Provincial Key Laboratory of Nuclear Science, Institute of Quantum Matter, South China Normal University, Guangzhou 510006, China.
[k]Also at MOE Frontiers Science Center for Rare Isotopes, Lanzhou University, Lanzhou 730000, People's Republic of China.
[l]Also at Lanzhou Center for Theoretical Physics, Lanzhou University, Lanzhou 730000, People's Republic of China.
[m]Also at the Department of Mathematical Sciences, IBA, Karachi 75270, Pakistan.
[n]Also at Ecole Polytechnique Federale de Lausanne (EPFL), CH-1015 Lausanne, Switzerland.
[o]Also at Helmholtz Institute Mainz, Staudinger Weg 18, D-55099 Mainz, Germany.
[p]Also at School of Physics, Beihang University, Beijing 100191, China.